Low Temperature Physics/Fizika Nizkikh Temperatur, 2019, v. 45, No. 7, pp. 881–891

Composite films of single-walled carbon nanotubes with strong oxidized graphene: characterization with spectroscopy, microscopy, conductivity measurements (5–291 K) and computer modeling

V.A. Karachevtsev, A.M. Plokhotnichenko, M.V. Karachevtsev, A.S. Linnik, and N.V. Kurnosov

B. Verkin Institute for Low Temperature Physics and Engineering of the National Academy of Sciences of Ukraine
47 Nauky Ave., Kharkiv 61103, Ukraine
E-mail: karachevtsev@ilt.kharkov.ua

Received February 5, 2019, published online May 28, 2019

The hybridization of 1D carbon nanotubes and 2D graphene family is able to form 3D nanostructures with significantly improved electrical, mechanical and thermal properties, which make them very useful for huge potential applications. In this work the graphene oxide-single walled carbon nanotube (GO-SWNT) hybrids prepared in aqueous suspension and films obtained by vacuum filtration are studied with UV–IR absorption spectroscopy, scanning electron microscopy (SEM) and computer simulation. Low-temperature measurements of conductivity of these films in the temperature range 5–291 K were also performed. For hybrid preparation SWNTs with prevailing content of semiconducting nanotubes (up to 95%) and graphene oxide with small C:O ratio (about 1.3) were selected. SEM analysis of a cutoff of the composite GO-SWNT film showed that the film is formed by composition of thin layers which are preferably located along the surface of the film with laminar, rather dense package. We have found spectroscopic manifestation of the interaction between GO and SWNT in the hybrid, estimated the interaction energy between components, revealed the conductivity in the composite film although in the GO film we have not observed a noticeable conductivity. It was also demonstrated that the behavior of the temperature dependence of the conductivity in the film of pure SWNTs and in the composite one is different. The decrease in the conductivity with lowering of temperature indicates that this dependence is similar with the conductivity observed in semiconducting systems.

Keywords: graphene oxide, single walled carbon nanotube, GO-SWNT hybrids, SWNT conductivity, UV–IR spectroscopy, computer simulation.

1. Introduction

Unique physical characteristics of graphene (Gr) such as an extremely high surface/mass ratio, high thermal conductivity which is higher than the thermal conductivity of copper, optical transparency in the visible range, high electron mobility, and others explain a huge attention of researchers to this nanomaterial. However, its chemical inertness and the difficulty of obtaining defect-free graphene sheets restrain its application in technology. Some scientists believe that these limitations can be removed by employing the oxidized and reduced forms of graphene [1,2]. Graphene oxide (GO) is a graphene with oxygen-containing groups at the edges (carboxyl-COOH and hydroxyl-OH groups) and on the plane (epoxy (C–O–C) and hydroxyl groups). Thus, GO has domains containing both sp^2-hybridized electrons of carbon atoms and sp^3-electron structures of carbon bound with oxygen-containing groups [1,2]. One of the main advantages of GO is its dispersibility in water, which expands the practical application of this nanomaterial, including its wide use for biological and medical purposes [3,4]. The reduced graphene oxide (rGO) has the predominantly sp^2-electronic structure, as after reduction (there is a wide range of different methods for reducing GO) a small amount of oxygen-containing groups remains. rGO can be considered a transitional nanomaterial between Gr and GO. Due to its solubility in water and partial restoration of hybridized electronic structure, that provides conductivity in sheets, rGO is a promising material for optoelectronics. The cost effective technological chain for obtaining carbon

material with physical properties close to graphene including *oxidation of graphite → production of graphene oxide → reduction of graphene oxide* makes rGO attractive for using in various fields of nanotechnology.

The combination of GO or rGO with various nanoparticles or nanotubes creates new hybrid nanomaterials with unique properties, first of all, optical and electronic ones. In these hybrid structures, there is an interleaving of rGO or GO sheets which are connected by carbon nanotubes or nanoparticles.

Significant progress has been made in the production of hybrids formed by carbon nanotubes (CNT) with Gr, rGO or GO [5]. In such hybrids, improved electrical, mechanical, and thermal properties were observed. To obtain films of CNT-rGO (or GO) hybrids, various methods are proposed: deposition from suspension under pressure (spray method), vacuum filtration, layer-by-layer deposition, and chemical vapor deposition. It is expected that this composite material has a significant potential for use as transparent conductive electrodes in solar cells, active electrodes in supercapacitors or in lithium-ion batteries.

CNTs are randomly distributed between rGO or GO sheets hybrids, and, therefore, provide a high mechanical strength and flexibility of such films. In such assembly, CNTs perform several functions: (1) preventing the Gr/rGO/GO sheets from re-sticking together in the films (forming films like a paper), (2) increasing conductivity between rGO/GO sheets, since CNTs have high electrical conductivity and can closely contact with the graphene surface, (3) ensuring more efficient conductive contact between the electrolyte and Gr/rGO sheets in a film.

It is known that single-walled CNTs (SWNTs) under normal conditions form bundles that are rather difficult to disperse in water or organic solvents. For their effective dispersion, several strategies are commonly used: chemical modification of the surface of nanotubes, the exploitation of surfactants or polymers [6]. The use of such additives reduces the electrical conductivity of the films obtained from suspensions since all of these dispersants are electrical insulators and therefore must be removed from the films obtained. This is a rather complex technological task, since the dispersants interact strongly with the nanotube surface and, as a result, they are difficult to remove. It turned out that GO can be used to disperse SWNTs. This approach has an important advantage: GO in the hybrid can be thermally/chemically reduced to produce rGO [1,2], which is electrically conductive, thereby the conductivity of the films are increased. Thus, GO can be used as a surfactant for dispersing SWNTs due to its solubility and high adhesion of nanotube to GO sheets through strong π–π interaction [7,8].

GO-SWNT films were obtained by several groups of researchers. For example, Tian *et al.* have obtained transparent conducting GO-SWNTs films when aqueous dispersions of SWNTs with GO were put onto glass substrates by a spray method [7]. Stable aqueous dispersion of hydrophobic SWNTs with small (nanoscale) sheets of GO were obtained by Dong with co-workers [8] without using any surfactants. It has been shown that nanoscale GO sheets are spontaneously wrapped around the SWNT bundles.

The hybrids of SWNTs with Gr/GO are used for the manufacture of fibers [9]. Hybrid fiber has demonstrated a synergistic increase in mechanical strength and electronic conductivity. Homogeneous hybrid transparent films consisting of GO and functionalized SWNTs were synthesized using a layer by layer process by means of the Langmuir–Blodget technique [10].

In this work we describe a preparation of the GO-SWNT hybrids in aqueous suspension and their films obtained by vacuum filtration from suspension and present results of the study of physical properties of these composite materials exploiting UV–IR absorption spectroscopy, scanning electron microscopy, computer simulation and temperature dependence measurements of the conductivity of SWNTs and composite films in the temperature range 5–291 K. The distinctive feature of our hybrids is that for hybrid preparation we have used the SWNTs with prevailing content of semiconducting nanotubes (up to 95%) and GO with small C:O ratio (about 1.3) that indicates the significant content of oxygen-containing groups in sheets. In our study we have shown spectroscopic manifestation of the interaction between GO and SWNT in the hybrid, estimated the interaction energy between components, revealed the conductivity in composite film while in GO film we have not observed a noticeable conductivity. We have also demonstrated that the behavior of the temperature dependence of the conductivity in the film of pure SWNTs and in the composite one is different. The decrease in the conductivity with temperature lowering indicates that this dependence is similar with the conductivity observed in semiconducting systems.

2. Experimental details

2.1. Materials

Graphene oxide used in our studies was purchased from Graphenea (San Sebastian, Spain). The GO was synthesized by chemical oxidation of graphite using the modified Hammers method [11]. In GO the content of carbon and oxygen was 49–56% and 41–50%, respectively (so the C/O ratio was 1.2–1.3). The SWNTs were purchased from SouthWest NanoTechnologies (USA). The nanotubes were grown by chemical vapor deposition method (CoMoCat method). The SWNT sample contained predominantly semiconducting nanotubes (~ 95%), among them, nanotubes of chirality (6,5) prevailed.

2.2. Preparation of GO-SWNT hybrids in aqueous suspensions

To obtain GO-SWNT hybrids we used stable aqueous suspension of GO (the initial concentration of GO was

~ 0.2 mg/ml), which was mainly in the form of monolayers [4]. The preparation method of aqueous suspensions of GO-SWNT hybrids is based on the ultrasound treatment (60 min) of the mixture of the aqueous suspension of GO monolayers with carbon nanotubes added to this suspension. The GO concentrations in suspension were ~ 0.2 mg/ml while the weight ratio of GO: SWNT was 4:1, 2:1 and 1:1.

2.3. Preparation of composite GO-SWNT films

The composite GO-SWNT films were obtained from aqueous suspension of GO-SWNTs (0.5–2 ml) deposited on the PTFE membrane (diameter 12.5 mm, pores 0.24 μm, Millipore, USA) by vacuum filtration. Subsequently, the GO-SWNT film was detached from the membrane and as a result circles (diameter ~ 9 mm) were prepared. An estimation of the composite density in the film gave the value 0.4–0.5 mg/cm^2. The GO films were obtained in a similar way.

2.4. Preparation of SWNT films

For the preparation of SWNT films, we also used the method of ultrasonication of nanotubes in acetone solution (nanotube concentration was ~ 0.2 mg/ml) during 40 min. The obtained suspension of nanotubes was deposited on the membrane by the vacuum filtration method (the density of the nanotube film was 0.3–0.4 mg/cm^2).

2.5. Experimental measurements

The absorption spectra of aqueous suspensions of GO, polynucleotide-wrapped SWNTs (prepared by ultrasonication with centrifugation, see for detail [12]) and GO-SWNT hybrids in the range of 200–1200 nm were recorded using two channels Hitachi-356 spectrometer (Hitachi, Japan). The IR absorption spectra of GO and GO-SWNTs in KBr pellets were recorded exploiting IR spectrometer (Specord-M80, Germany) in the spectral range of 500–4000 cm^{-1}. The surface morphology of films obtained by vacuum filtration was analyzed using a JSM-820 scanning electron microscope (JEOL, Japan).

To verify linear or nonlinear character the volt-ampere dependence for the obtained films was studied using an automated set-up. The conductivity was determined from the film in the form of the square with a side of 6 mm using a mechanical stiffener. The low-temperature measurements of the film conductivity in the range 5–291 K were carried out in a helium cryostat with temperature stabilization of the film kept in the gas helium atmosphere. Measurements of the conductivity of the films were carried out both during the film cooling and heating simultaneously for SWNTs and GO-SWNT films. The average rate of temperature changes was about 1.5–2 K/min.

2.6. Molecular dynamics modeling

In the computer simulation, a short SWNT with (10,0) chirality (diameter of 0.79 nm) and a length of 10 nm (960 carbon atoms and 20 hydrogen atoms for termination of tube ends) was used. A graphene sheet with the size of 7×1.16 nm (462 carbon atoms, 72 hydrogen atoms for termination of graphene edge) was located at a distance of 4 Å from the surface of SWNT. It should be noted that all atoms of the graphene sheet were in the same plane. At the initial stage of modeling, graphene was located above the nanotube surface, in such way that the longer side of graphene sheet was perpendicular to the nanotube axis. Further, the entire system was placed in a water box of 108×36×96 Å (11315 water molecules). Molecular dynamics simulation was performed using the NAMD program [13] with the Charmm force field [14]. Throughout the simulation, the number of atoms, pressure and temperature in the system were unchanged (NPT approach). To account for the electrostatic interaction, the Particle Mesh Ewald [15] method was used. The total simulation time was 10 ns, the simulation step was 1 fs. For visualization of the simulated nanostructures, the software package VMD [16] was used.

3. Results and discussion

3.1. Bending strength and surface morphology of composite films obtained by vacuum filtration

Vacuum filtration is a fairly simple but effective method for producing films by permeation of nanoparticle suspension (in water or organic solvent) through a membrane. This method has several advantages: obtaining a sufficiently uniform film with thickness control and with high effectiveness of material using, the simple and cost effective procedure to fabricate a membrane that can occur gas or liquid thin filtration. Figure 1 shows photography of the composite GO-SWNT film obtained by this method. Even visually, it is seen that light reflection indicates a smooth surface of the composite film. Knowledge of the concentration and the volume makes it possible to estimate the thickness of the film; in our films it was in the range of 1–10 μm. These films of carbon nanomaterials can be lightly separated from the filter without breaking after drying. The photography shown in the right part of Fig. 1 demonstrates a high flexibility and elasticity of the composite film that can be easily

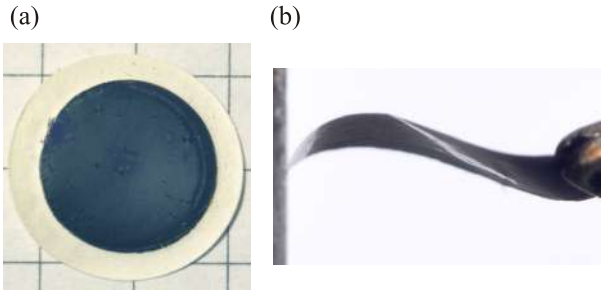

Fig. 1. (a) GO-SWNT film on PTFE membrane obtained by vacuum filtration (thickness is about 1–4 μm). (b) A flexibility and elasticity of the composite film that can be easily twisted without rupture.

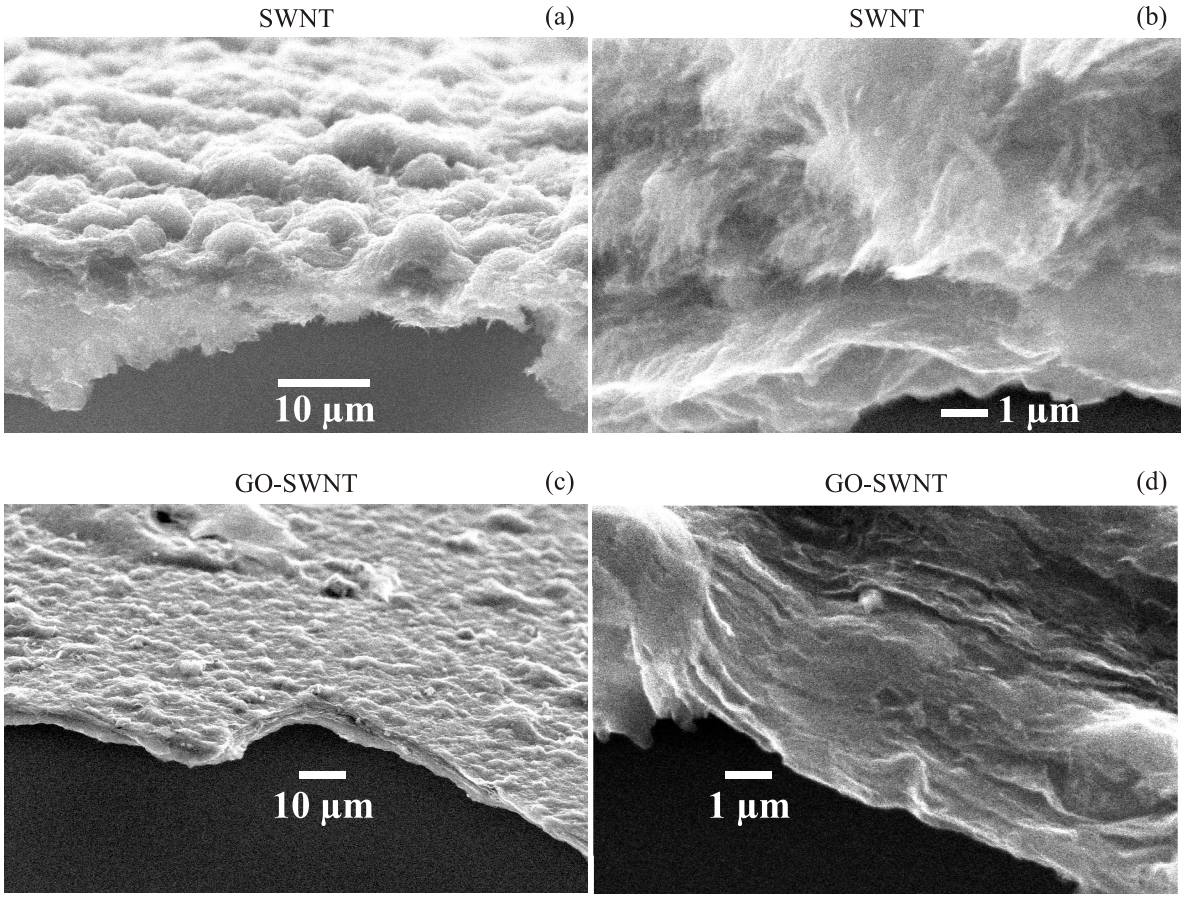

Fig. 2. SEM images of surfaces of carbon nanotubes (upper part) and composite GO-SWNT (lower part) films (the 10 μm scale is indicated on images of each film) and the cutoff of these films (right images, the scale is 1 μm).

twisted without rupture. It should be noted that the composite film has a high porosity; we observed a permeability of water through the film with the thickness above 10 μm. In contrast to this composite film the GO films were impermeable for water if the thickness of the film was above 4–5 μm.

SEM images of the surface of the carbon nanotubes (upper part) and the composite GO-SWNT (lower part) films are shown in Fig. 2 (left), the 10 μm scale is indicated on images of each film. We can see a dense, but rather rough surface, obtained due to the solvent filtration. Note, that a roughness of the composite film surface is less than it is observed for the nanotube one. A microscopic image of each film cutoff is shown in the right part of Fig. 2 with a significant magnification, the scale is 1 μm. From this cutoff the thickness of the films can be estimated which is close to 10 μm. SEM analysis of the cutoff of the composite GO-SWNT film shows that the film is formed by composition of thin layers (like papers) which are preferably located along the surface of the film with laminar, rather dense package. The different distances between these layers in the film suggest its porosity. In contrast to this film a more chaotic structure in volume is observed for the nanotube one (Fig. 2, top, right).

3.2. Absorption spectroscopy of GO-SWNT hybrids in aqueous suspension: UV-visible-near IR spectral range

The absorption spectrum of GO-SWNT hybrids in aqueous suspension in the range of 200–1200 nm is shown in Fig. 3 (the concentration ratio of the components is 0.2:0.5 mg/ml). Suspension was prepared by ultrasonication for 40 min. For comparison the absorption spectrum of GO suspension is also shown in this figure.

Both spectra have similarity and are characterized by intensive asymmetrical band in UV range which shows a significant increase in light absorption with a decrease in wavelength. This absorption is due to the plasmon absorption of light, which is characteristic of the carbon systems [6]. The UV spectrum of hybrids has two features: the absorption peak at 220–240 nm due to the transition of $\pi \rightarrow \pi^*$ electrons in carbon atoms, which form sp^2 hybridization (C=C bond), and a shoulder at 280–320 nm, which is associated with the $n \rightarrow \pi^*$ electron transition of carbon in the C=O group (sp^3-electron hybridization) (see, for example, [4]). While the first peak is observed for the both components of the hybrid, the second one is characteristic feature of GO only. In spite of the visible similarity of GO and GO-

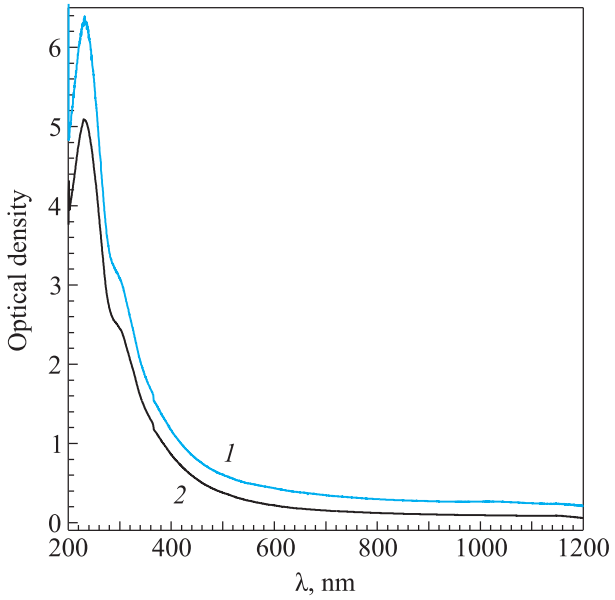

Fig. 3. The absorption spectrum of GO-SWNT hybrids (*1*) in aqueous suspensions (the concentration ratio of the components was 0.2:0.5 g/l) and the GO absorption spectrum (*2*). The spectra were normalized to the same length of the optical path (5 mm).

SWNT spectra, the more detailed analysis shows the difference. To clearly show it we have subtracted the spectrum of GO from the GO-SWNT spectrum providing the same concentration of GO in both suspensions. Figure 4 shows the resulting differential spectrum in the range of 400–1200 nm.

In the differential spectrum, one can see the bands that correspond to the absorption spectrum of nanotubes located in hybrids. For comparison, in this figure the nanotube spectrum of the aqueous suspension of individual nanotubes with adsorbed homopolynucleotide (poly(rC)) is shown as well. It is known that the biopolymer provides a stable aqueous suspension of individual nanotubes [6]. The poly(rC)-wrapped SWNT spectrum is characterized by the presence of bands in the range of 400–1200 nm, which are more intensive and narrow than those in the differential spectrum. The bands in the 450–800 nm range correspond to E_{22} transitions in semiconducting nanotubes (transition between the second van Hove singularities in the valence and conductance bands, $v_2 \rightarrow c_2$) (see, for example, review [6]). The bands in the 800–1200 nm range correspond to E_{11} transitions (between the first van Hove singularities, $v_1 \rightarrow c_1$) in semiconducting nanotubes. The most intensive band in the spectrum of SWNTs (CoMoCat) is assigned to nanotubes with the (6,5) chirality (the band at 993 nm) [12].

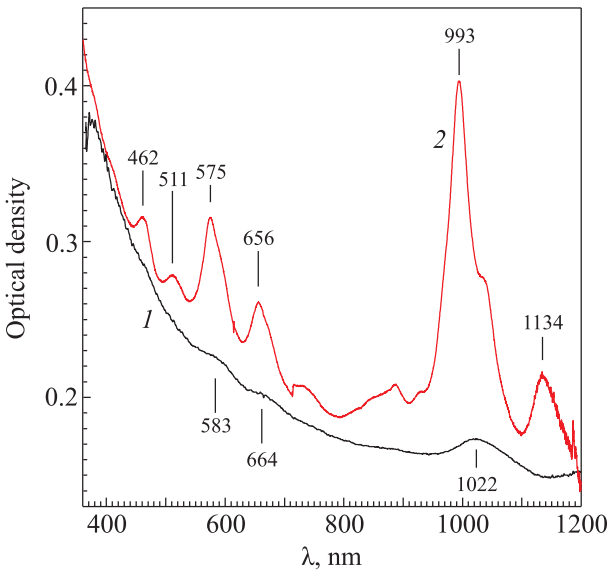

Fig. 4. The differential absorption spectrum of nanotubes in hybrids (*1*) obtained by subtraction the spectrum of GO from the GO-SWNT spectrum and the absorption spectrum of aqueous suspensions of SWNTs covered by poly(rC) (*2*).

The comparison of the peak positions of the two spectra has shown the 2–8 nm red shift for bands corresponding to nanotube E_{22} transitions in the hybrids as compared with the spectrum of the nanotubes covered with poly(rC). The red shift is more significant for bands assigned to E_{11} transitions in semiconducting nanotubes. We should also note the significant weakening of the band intensity as well as increasing of the nanotube bandwidths in the hybrids. Thus, the interaction of carbon nanotubes with graphene oxide is accompanied by the red shift and broadening of absorption bands of nanotubes, as well as a significant weakening of the intensity of the bands associated with E_{11} and E_{22} electronic transitions in semiconducting nanotubes. Quenching of the E_{11} and E_{22} absorption bands indicates an electron withdrawal from the semiconducting SWNTs in the film [17].

3.3. Characterization of GO-SWNT hybrids: IR spectroscopy

IR absorption spectrum of GO-SWNT hybrids in KBr pellet in the range of 4000–400 cm^{-1} is shown in Fig. 5. The IR absorption spectrum of GO is also presented in this figure for comparison. The IR absorption spectra of GO and its hybrid are characterized by the presence of several intensive absorption bands in the range of 3500–400 cm^{-1}. In the high-frequency region at the frequency of 3400–3300 cm^{-1}, an intense broad band is observed caused by vibrations of the O–H groups (Fig. 5). It should be noted that a KBr pellet contains some amount of water and hydrocarbons molecules adsorbed from air. In the IR spectrum, relatively broad bands attributed to water molecules appears near 3600–3200 and 1660–1590 cm^{-1}. The hydrocarbon bands can be observed in the IR spectrum mainly as relatively narrow bands at 2920–2850 cm^{-1}. The spectra of GO-SWNTs and GO showed in Fig. 5 were obtained by subtracting the impurity spectrum (the "empty" KBr pellet) from the spectrum observed for each sample in KBr pellet. Such correction made it possible to almost completely remove the water bands that are in the KBr pellet.

Note that the detailed information on GO can be obtained by analyzing the absorption spectrum in the range of

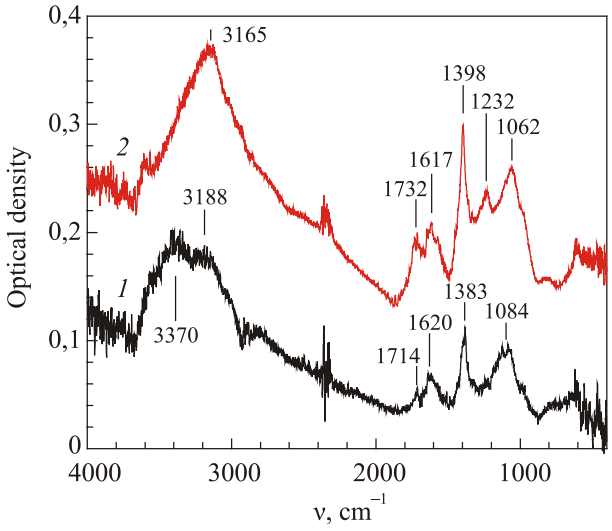

Fig. 5. IR absorption spectra of GO-SWNT hybrids (*1*) and GO (*2*) in KBr pellets. Numbers indicated near some bands correspond to wave number of the peak position (in cm^{-1}). For better visualization the spectra are shifted along the intensity axis.

1800–500 cm^{-1} where bands corresponding to the vibrations of different oxygen-containing groups as well as graphene hexagons are located (see Ref. 4 and references therein). The band in the spectrum at the frequency of 1732 cm^{-1} is due to the stretching vibration of the carbonyl groups ν(C=O). This band is the main spectral characteristic of the GO sheets. The bands located in the range of 1650–1580 cm^{-1} are associated with vibrations of carboxyl groups and C=C vibrations characteristic for the sp^2 domains. The most intensive band at the frequency of 1398 cm^{-1} in the GO spectrum is assigned to the deformation vibrations of hydroxyl (O–H) group. Vibrations of the epoxy group (C–O–C) make a significant contribution to absorption at the frequency of 1232 cm^{-1}. The broad absorption band in the frequency range of 1100–1000 cm^{-1} with the peak at 1062 cm^{-1} is associated mainly with the vibrations of the C–O group of furan-like ethers and hydroxyl group.

As can be seen from Fig. 5 the IR absorption spectrum of the GO-SWNT hybrids differs from the spectrum of pure GO. First of all, we note the lower intensity of the entire IR spectrum of GO-SWNTs. The spectrum contains an intense vibration band of water molecules at a frequency of 3370 cm^{-1}, which manifests itself despite of the above-described correction of the spectrum for water absorption. In the region of 1800–1000 cm^{-1} some changes in the frequencies and intensities of the spectral bands are observed in the hybrid spectrum as compared to the GO spectrum. These changes are primarily due to the appearance of the interaction between two carbon nanomaterials. It includes the interaction of π–π systems of nanotubes and GO (through the sp^2 domains), and the interaction of oxygen-containing groups of GOs with the π system of nanotubes. In addition, the structural features of the obtained composite should be taken into account, namely, its high porosity. The thin cavities between the GO sheets separated by nanotubes may contain a significant amount of water molecules that does not evaporate even when the composite is dried. This water manifests itself in the IR spectrum directly, but it can significantly change the GO spectrum due to the formation of hydrogen bonds with oxygen-containing groups of GO. High porosity of GO-SWNT composite film is also confirmed by the fact of high permeability of water by the GO-SWNT composite film on PTFE filter at the film thickness up to 15 μm.

A significant shift towards lower frequencies of some bands should be noted (1732 → 1714 cm^{-1}, 1398 → → 1383 cm^{-1}), but the bands characterizing the C=C vibrations of the aromatic fragments of GO are shifted towards higher frequencies (1617 → 1620 cm^{-1}). This blue shift of the band due to C=C vibrations in hexagons indicates the interaction of carbon nanotubes with the sp^2 domains of GO. It should be noted that this blue shift can be also caused by the appearance of curvature of GO sheets as a consequence of embedding of rods (nanotubes) between them. The vibrations associated with oxygen-containing groups also demonstrate the manifestation of the interaction between GO and SWNTs.

Thus the observed spectral shifts of the band associated with C=C vibrations in the sp^2-hybridized domain of GO as well as bands assigned to oxygen-containing groups indicate the interaction of carbon nanotubes with the GO surface.

3.4. Interaction of single-walled carbon nanotube with graphene: molecular dynamics study

We simulated the process of forming the hybrid of SWNT with graphene by molecular dynamics to evaluate the interaction between the components and to study the influence of water on the interaction between graphene and carbon nanotube.

In the calculations we have used the (10,0) SWNT and a graphene sheet in the form of rectangular strip with size of 7×1.16 nm. At the initial stage of the simulation the SWNT was located above the center of the graphene sheet at a distance of 4 Å, as shown in Fig. 6(a). Then the system was placed in a water box.

The structures of the SWNT hybrid with graphene after the completion of the simulation are shown in Fig. 6(b). The analysis of the structure shows that the hybrid remains stable during the whole simulation time. The interaction between the components of the hybrid leads to turn of the sheet by about 90° relative to the initial position. It should be noted that the graphene reorientation occurs in the first 2.5 ns simulation, and during the later simulation period this graphene arrangement relative to nanotube remains almost unchanged, only insignificant thermal fluctuations are observed. We note that in the obtained hybrid some graphene atoms displace from the plane and the graphene sheet is distorted.

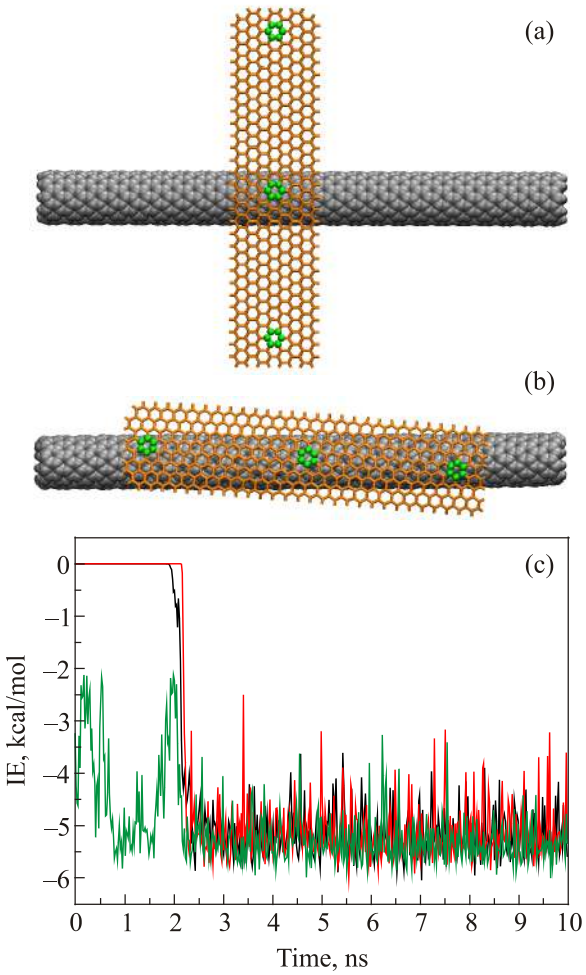

Fig. 6. (Color online) Structure of SWNT and graphene sheet in front (a) and side (b) views. The dependence of the interaction energy between graphene sheet and marked hexagons indicated in (a), (b) on the simulation time is shown in the lower part of the Fig. 6(c).

It is obvious, that the parallel orientation of the graphene sheet relative to the SWNT axis provides the maximum area of contact between the components of the hybrid, so the resulting configuration is more energetically favorable than the starting one. In order to consider this turn in more detail, the energy of the interaction between SWNT and graphene was monitored during simulation. The dependence of the binding energy on the simulation time is shown in Fig. 7. It can be seen that from the very beginning of the simulation, the interaction energy between graphene and SWNT is gradually increasing from –66 to –95 kcal/mol up to 1.75 ns. Thereafter, a sharp increase in the energy of interaction to ≈ 265 kcal/mol occurs, this growth continues only for 0.5 ns, but during this energy growth the graphene sheet is re-orientated. For the rest 7.5 ns simulations, no significant changes in the energy of interaction are observed, therefore, we can conclude that after the first 2.5 ns simulation the system becomes stable.

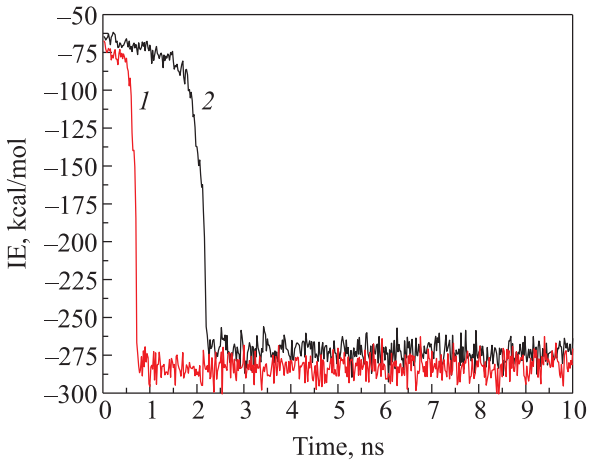

Fig. 7. The dependence of the interaction energy between SWNT and the graphene sheet on the simulation time in vacuum (*1*) and in water environment (*2*).

We have estimated the binding energy of one hexagon of graphene with the nanotube surface. For this purpose we select three hexagons located in different parts of the graphene sheet: one hexagon is fixed in the center and two others placed on different edges of the graphene sheet, as shown in Fig. 6(a). The simulation showed that after 10 ns each of hexagons interacts with the SWNT surface with comparable energy, as shown in Fig. 6(c). After 2.5 ns simulation all three hexagons have the energy about –5.3 kcal/mol with fluctuations up to 1.5 kcal/mol. Note that the significant difference in the energy is observed only in the first nanoseconds of simulation, so the hexagons located on the edges of graphene almost do not interact with the SWNT, however, after 2 ns of simulation there is a sharp increase in the energy up to ~ –5 kcal/mol. For the hexagon located in the center of graphene sheet the energetically favorable binding with SWNT occurs at the first simulation steps. It is necessary to note the presence of essential oscillations spanning ~ 3 kcal/mol, but they decay after 2 ns when the optimal arrangement of graphene on SWNT is set. Note that quantum-chemistry calculations of the interaction energy of benzene molecule with SWNT [18] or graphene [19] gave slightly larger energy value. Thus, the binding energies of benzene with the zigzag (10,0) and armchair (6,6) nanotube surfaces are –7.5 and –6.7 kcal/mol, respectively, while for the graphene surface this energy has a value in the range of –(5.9–8.4) kcal/mol depending on the benzene ring arrangement over a graphene hexagon [19].

Since one of the factors that stabilizes the structure of the graphene-SWNT hybrid is a water environment, it would be very interesting to study in more detail the influence of water on the structure of the hybrid and on the interaction energy between components. For this purpose, the graphene-SWNT hybrid was simulated in vacuum too. The total simulation time was 10 ns. The graphene-SWNT hybrid structure in vacuum after 10 ns simulation nearly did not differ from the structure of the hybrid in water en-

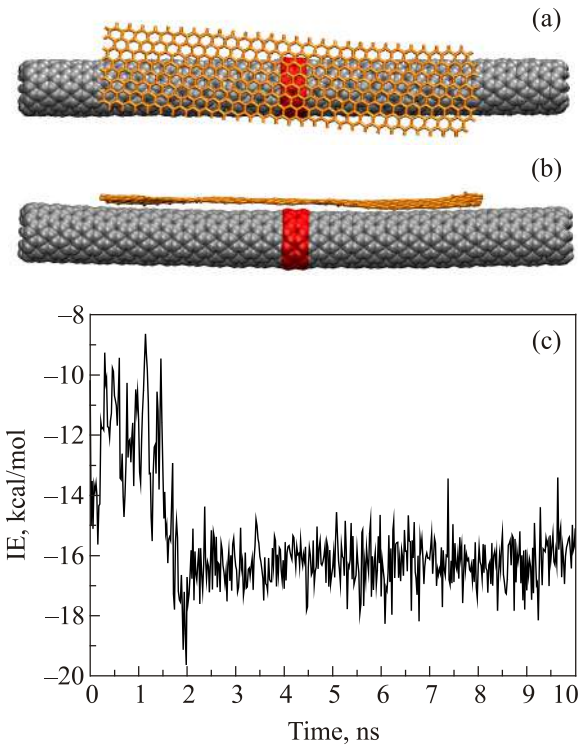

Fig. 8. Structure of SWNT-graphene in front (a) and side (b) views. The dependence of the interaction energy (c) between hexagon belt of SWNT indicated in (a) and graphene on the simulation time.

vironment, but it should be noted that the rate of graphene reorientation to reach maximal binding is increased. In vacuum, the turn of the graphene sheet occurs during the first nanosecond of simulation, while in water environment this re-orientation takes 2.5 ns (Fig. 7). In general, the binding energy after 2 ns of simulation for the system in vacuum is about –282 kcal/mol (2–10 ns), while for the system in water environment this energy is about –273 kcal/mol (3–10 ns). The interaction energy in the case of the graphene-SWNT hybrid in vacuum is higher by about –10 kcal/mol in comparison with the water environment. Therefore, it can be concluded that the water environment slows down and prevents graphene from occupying the favorable position relative to the carbon nanotube and slightly decreases the binding energy.

We have also determined the interaction energy of graphene with nanotube hexagons which form a belt around nanotube (Figs. 8(a),(b)). This energy value, naturally, depends on the nanotube diameter. In our case, for relatively narrow nanotube (diameter of 0.79 nm), this value reaches up ~ 16 kcal/mol after graphene sheet turning (after 2 ns simulation). In spite of that this value was estimated for 8 nanotube hexagons in the belt, this energy is only three times larger than the interaction energy of one hexagon stacked with graphene. This value gives opportunity to estimate the binding energy of graphene with such nanotube of any length.

3.4. Temperature dependence of conductivity of GO-SWNT composite film compared with SWNT film

The films of carbon nanomaterials obtained by vacuum filtration exhibit different electrical conductivities, namely, GO films are practically non-conducting, while it is observed in composite GO-SWNT films. The appearance of the conductivity in composite films is obviously associated with the addition of SWNTs, since films of carbon nanotubes show a fairly high conductivity. Note that in the composite film with thickness of about 4 μm and with GO:SWNT weight ratio of 4:1 we did not observed a noticeable conductivity which appears in the film with weight ratio of 2:1.

The temperature dependences of the conductivity (σ(*T*)) of the GO-SWNT and SWNT films in the range of 5–291 K are shown in Fig. 9. Note, that at the starting high temperature (291 K) the conductivity of the SWNT film has a larger value than it was observed for the composite film (more than in 20 times). Measurements of the electrical conductivity of the films were carried out both during the film cooling and heating, no hysteresis between dependences was observed. As it follows from the figure the conductivity of both films decreases with temperature lowering, but the curves of this dependence for the films are different. So, for SWNTs, the σ(*T*) curve shows a smaller slope, however, at $T < 70$ K a rapid fall in the conductivity occurs. For the composite film, the dependence shows a more uniform decrease in the conductivity with temperature lowering. The similar temperature dependence, namely, decrease in conductivity with temperature lowering is observed in semiconducting systems [20]. It is obvious that the conductivity of the composite film is mainly determined by the

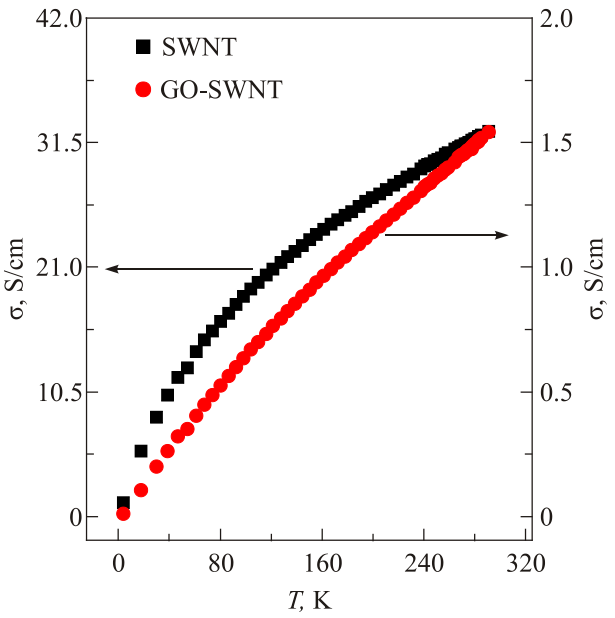

Fig. 9. The temperature dependences of the conductivity σ(T) of GO-SWNT (circles) and SWNT (squares) films in the range of 5–291 K.

nanotubes. According to different behaviors of the temperature dependency, we can conclude that the presence of GO also affects the electrical conductivity in the composite film. This may be due to the fact that in the composite film the nanotubes are in contact with sp^2-hybridized domains that are on the GO sheet. These domains do not provide the conductivity through the GO sheet or film, but they can affect the conductivity through nanotubes acting as bridges between them. On the contrary, domains with sp^3-electrons can create additional barriers to the transport of electrons. The interaction of carbon nanotubes with GO also influences on barriers for electrons tunneling that form nanotubes (or nanotube bundles) in crossing points.

Electrical conductivity in SWNTs, in individual nanotubes, bundles, nanotube networks, thin and bulk films has been studied quite well (see reviews [20,21]). However, despite numerous studies of the conductivity of the SWNT networks or films, a selection of the fundamental mechanism (model) of the electron transport to describe the temperature dependence still remains an incompletely clarified task. The model selection depends on many factors, primarily on the type of the conductivity in individual nanotubes, as well as their length and diameter, the ratio of metallic nanotubes to semiconducting ones, and the level of their chemical doping. Peculiarities of the nanotube networking which can be formed by individual nanotubes or by their bundles, as well as the degree of nanotube alignment along one direction also influence on the conductivity of the nanotube system. Note that the conductivity of nanotube bulk films depends also on the film thickness [22]. The nanotube conductivity was studied in fibers in which bundles are aligned along one direction and in films of nanotubes in a polymer environment [20,21]. It is clear that each type of sample studied introduces its characteristics into the electrical conductivity mechanism of the film/network of carbon nanotubes. The basic mechanism that explains the conductivity in carbon nanotube systems at low temperatures is determined by the tunneling of thermally activated electrons through barriers formed by contacts between nanotubes. At higher temperatures this mechanism is supplemented with the electron hopping over barriers.

In experimental studies, the temperature dependence of the resistance of the carbon nanotubes film/network is often measured. Two basic models are used to describe this dependence, and, therefore, the main transport mechanism in the SWNT films: fluctuation-induced tunneling (FIT) suggested by Sheng [23,24] and a variable-range hopping (VRH) model elaborated by Mott [25].

The FIT model states that the conductivity in such system is determined by the tunneling of thermally activated electrons through barriers formed by contacts between nanotubes, while the barrier height for tunneling decreases due to fluctuation effects. In the VRH model, which successfully explains the transport behavior of charges in disordered systems, it is indicated that thermally activated electrons hop from one localized level near the Fermi level (E_F) to another local level. At sufficiently low temperatures, the energy transfer is weakened and the electron hops at greater distance to a state with an energy close in magnitude to the initial one. In this model, it is often assumed that the density of states near E_F is constant. Despite the difference in the theoretical description, the physics of the process in both FIT and VRH approaches involves the tunneling of charge carriers between the electronic states near the Fermi level.

Since carbon networks [25] and GO due to oxygen-containing group decoration [26,27] are considered as disordered carbon materials so our films studied should be regarded as disordered semiconducting system.

4. Conclusions

Composite GO-SWNT films fabricated by vacuum filtration are solid, dense and flexible. The film surface has a roughness that is formed due to solvent filtration. SEM analysis showed that the composite GO-SWNT film is formed by composition of thin layers which are preferably located along the surface of the film with laminar, rather dense package. A different distance between the layers indicates the film porosity confirmed by solvent permeability.

The interaction energy of graphene hexagons stacked with the SWNT surface estimated by molecular dynamics simulation has the value of about –5.3 kcal/mol. It is shown that in the water environment this energy is approximately 4% less than in vacuum. The water environment also slows down the acquisition of the energetically favorable conformation for the graphene-SWNT structure. The interaction between GO and SWNT leads to the absorption spectrum transformation accompanied with red shifting and broadening of some bands in the visible-NIR region (electronic transitions) and in IR absorption spectra.

The composite films show the conductivity although GO films are practically non-conducting. It was demonstrated that the behavior of the temperature dependence of the conductivity in film of pure SWNTs and in the composite one is different. The decrease in the conductivity with temperature lowering from 291 to 5 K indicates that the behavior is similar with the conductivity dependence observed in disordered semiconducting systems.

The fabricated 3D carbon nanostructures formed by nanotubes and graphene oxide show significantly improved electrical conductivity of GO, which make them very useful for many potential applications such as production of supercapacitors and lithium batteries, layering conductive and transparent coverage, production of filters for water purification and so on.

5. Acknowledgments

This work was supported by the National Academy of Sciences of Ukraine (NASU) (Grant N 15/19-H within the program “Fundamental Problems of the Creation of New

Nanomaterials and Nanotechnology", Grant N 07-01-19 and Grant N 0117U002287). M.V.K. and N.V.K. acknowledge support from the NASU: Grant N 1/H-2019. The authors acknowledge the Computational Center at B.I. Verkin Institute for Low Temperature Physics and Engineering for providing computer time. We are grateful to P.V. Mateichenko for SEM measurements.

1. C.K. Chua and M. Pumera, *Chem. Soc. Rev.* **43,** 291 (2014).
2. R.K. Singh, R. Kumar, and D.P. Singh, *RSC Adv.* **6**, 64993 (2016).
3. S.S. Nanda, G.C. Papaefthymiou, and D.K. Yi, *Crit. Rev. Solid State Mater. Sci.* **40**, 291 (2015).
4. M.V. Karachevtsev, S.G. Stepanian, A.Yu. Ivanov, V.S. Leontiev, V.A. Valeev, O.S. Lytvyn, L. Adamowicz, and V.A. Karachevtsev, *J. Phys. Chem. C* **121**, 18221 (2017).
5. H.X. Kong, *Curr. Opin. Solid State Mater. Sci.* **17**, 31 (2013).
6. I.A. Levitsky, W.B. Euler, and V.A. Karachevtsev, *Photophysics of Carbon Nanotubes Interfaced with Organic and Inorganic Materials*, Springer-Verlag, London (2012).
7. L.L. Tian, M.J. Meziani, F. Lu, C.Y. Kong, L. Cao, T.J. Thorne, and S. Ya-Ping, *ACS Appl. Mater. Interf.* **2**, 3217 (2010).
8. X. Dong, G. Xing, M.B. Chan-Park, W. Shi, N. Xiao, J. Wang, Q. Yan, T.C. Sum, W. Huang, and P. Chen, *Carbon* **49**, 5071 (2011).
9. R. Wang, J. Sun, L. Gao, C. Xu, and J. Zhang, *Chem. Commun.* **47**, 8650 (2011).
10. Q. Zheng, B. Zhang, X. Lin, X. Shen, N. Yousefi, Z.-D. Huang, Z. Li, and J.-K. Kim, *J. Mater. Chem.* **22,** 25072 (2012).
11. W.S. Hummers, Jr., and R.E. Offeman, *J. Am. Chem. Soc.* **80**, 1339 (1958).
12. N.V. Kurnosov, V.S. Leontiev, A.S. Linnik, O.S. Lytvyn, and V.A. Karachevtsev, *Chem. Phys.* **438**, 23 (2014).
13. J.C. Phillips, R. Braun, W. Wang, J. Gumbart, E. Tajkhorshid, E. Villa, Ch. Chipot, R.D. Skeel, L. Kale, and K. Schulten, *J. Comput. Chem.* **26**, 1781 (2005).
14. N. Foloppe and A.D. MacKerell, Jr., *J. Comput. Chem.* **21**, 86 (2000).
15. U. Essmann, L. Perera, M.L. Berkowitz, T. Darden, H. Lee, and L.G. Pedersen, *J. Chem. Phys.* **103,** 8577 (1995).
16. W. Humphrey, A. Dalke, and K. Schulten, *J. Molec. Graphics* **14**, 33 (1996).
17. I. Puchades, C.C. Lawlor, C.M. Schauerman, A.R. Bucossi, J.E. Rossi, N.C. Cox, and B.J. Landi, *J. Mater. Chem. C* **3**, 10256 (2015).
18. E. Zarudnev, S. Stepanian, L. Adamowicz, V. Leontiev, and V. Karachevtsev, *Chem. Phys.* **483–484**, 68 (2017).
19. E.S. Zarudnev, S.G. Stepanian, L. Adamowicz, and V.A. Karachevtsev, *Chem. Phys. Chem.* **17**, 1204 (2016).
20. A.B. Kaiser and V. Skakalova, *Chem. Soc. Rev.* **40**, 3786 (2011).
21. L. Hu, D.S. Hecht, and G. Gruner, *Chem. Rev.* **110**, 5790 (2010).
22. V. Skakalova, A.B. Kaiser, Y.-S. Woo, and S. Roth, *Phys. Rev. B* **74**, 085403 (2006).
23. P. Sheng, *Phys. Rev. B* **21**, 2180 (1980).
24. P. Sheng, E.K. Sichel, and J.I. Gittleman, *Phys. Rev. Lett.* **40**, 1197 (1978).
25. N.F. Mott and E.A. Davis, *Electronic Processes in Non-Crystalline Materials*, Oxford, Clarendon Press, New York (1979).
26. C.Y. Cheah and A.B. Kaiser, *Intern. J. Nanotechn.* **11**, 412 (2014).
27. R. Cheruku, D.S. Bhaskaram, and G. Govindaraj, *J. Mater. Sci. Mater. Electron.* **29,** 9663 (2018).

Композитні плівки одностінних вуглецевих нанотрубок з сильно окисненим графеном: характеризація за допомогою спектроскопії, мікроскопії, вимірювання електропровідності (5–291 K) та комп'ютерного моделювання

В.О. Карачевцев, О.М. Плохотніченко, М.В. Карачевцев, О.С. Ліннік, М.В. Курносов

Гібридизація вуглецевих нанотрубок (1D структури) з графеном або його похідними (2D структури) призводить до утворення 3D наноструктур, які мають покращені електричні, механічні та термічні властивості у порівнянні з компонентами, що відкриває широкий спектр їх практичного застосування. Гібриди одностінних вуглецевих нанотрубок (SWNT) з оксидом графена (GO), які приготовлені у водній суспензії, та плівки, що отримані вакуумною фільтрацією, досліджено із застосуванням УФ–ІЧ спектроскопії поглинання світла, скануючої електронної мікроскопії (СЕМ), комп'ютерного моделювання. Також виконано низькотемпературні вимірювання електропровідності плівок в інтервалі температур 5–291 K. Для приготування гібридів обрано SWNT з переважаючим вмістом напівпровідникових нанотрубок (до 95%) та оксиду графену з невеликим співвідношенням C:O (близько 1,3). СЕМ-аналіз зрізу композитних плівок GO-SWNT показав, що плівка складається з тонких шарів, які розташовані уздовж поверхні плівки з ламінарною, досить щільною упаковкою. Ми виявили спектроскопічний прояв взаємодії GO і SWNT у гібриді, оцінили енергію взаємодії між компонентами, виявили провідність у композитної плівці, хоча в плівці GO провідність практично не спостерігалася. Також було показано, що поведінка температурної залежності провідності в плівці SWNT та в композитній плівці різна. Зменшення провідності з пониженням температури вказує на те, що ця залежність аналогічна провідності, що спостерігається в напівпровідникових системах.

Ключові слова: оксид графену, одностінна вуглецева нанотрубка, гібриди GO-SWNT, провідність SWNT, УФ–ІК спектроскопія, комп'ютерне моделювання.

Композитные пленки одностенных углеродных нанотрубок с сильно окисленным графеном: характеризация с помощью спектроскопии, микроскопии, измерения электропроводности (5–291 К) и компьютерного моделирования

В.А. Карачевцев, А.М. Плохотниченко,
М.В. Карачевцев, А.С. Линник, Н.В. Курносов

Гибридизация углеродных нанотрубок (1D структуры) с графеном или его производными (2D структуры) приводит к образованию 3D наноструктур, которые обладают улучшенными электрическими, механическими и термическими свойствами в сравнении с исходными компонентами, что открывает широкий спектр их практического применения. Гибриды одностенных углеродных нанотрубок с оксидом графена (GO-SWNT), приготовленные в водной суспензии, и пленки, полученные вакуумной фильтрацией, исследованы с применением УФ–ИК спектроскопии поглощения света, сканирующей электронной микроскопии (СЭМ), компьютерного моделирования. Также выполнены низкотемпературные измерения электропроводности пленок в интервале температур 5–291 К. Для приготовления гибридов выбраны SWNT с превалирующим содержанием полупроводниковых нанотрубок (до 95%) и оксида графена с небольшим отношением C:O (около 1,3). СЭМ-анализ среза композитной пленки GO-SWNT показал, что пленка состоит из тонких слоев, расположенных вдоль поверхности пленки с ламинарной, довольно плотной упаковкой. Мы выявили спектроскопическое проявление взаимодействия GO и SWNT в гибриде, оценили энергию взаимодействия между компонентами, обнаружили электропроводность в композитной пленке, хотя в пленке GO проводимость практически не наблюдалась. Также было показано, что в пленке SWNT и в композитной пленке поведение температурной зависимости проводимости различно. Уменьшение проводимости с понижением температуры указывает на то, что эта зависимость аналогична наблюдаемой в полупроводниковых системах.

Ключевые слова: оксид графена, одностенная углеродная нанотрубка, гибриды GO-SWNT, проводимость SWNT, УФ–ИК спектроскопия, компьютерное моделирование.